



## Review Article

# Towards the application of 2D metal dichalcogenides as hydrogen evolution electrocatalysts in proton exchange membrane electrolyzers

Alexey Y. Ganin and Mark D. Symes

**Abstract**

The electrolysis of water using renewable power inputs has tremendous potential for storing renewable energy in the form of hydrogen fuel. Proton exchange membrane electrolyzers are amongst the more promising classes of electrolyzer for renewables-driven hydrogen production, but these devices require expensive and scarce precious metal electrocatalysts (such as platinum) that add considerably to device costs and lifecycle carbon footprints. Replacing platinum in proton exchange membrane electrolyzers with cheaper and more abundant alternatives will thus make renewables-to-hydrogen devices more viable. Two-dimensional metal dichalcogenides have the required stability, electronic and catalytic properties to challenge platinum's position as the electrocatalyst of choice in proton exchange membrane electrolyzers. In this minireview, we give an overview of recent progress in the development of two dimensional metal dichalcogenides as hydrogen evolution electrocatalysts, with a particular focus on studies from the last two years.

**Addresses**

WestCHEM, School of Chemistry, University of Glasgow, Glasgow, G12 8QQ, United Kingdom

Email address: [alexey.ganin@glasgow.ac.uk](mailto:alexey.ganin@glasgow.ac.uk) (A.Y. Ganin), [mark.symes@glasgow.ac.uk](mailto:mark.symes@glasgow.ac.uk) (M.D. Symes)

**Current Opinion in Electrochemistry** 2022, **34**:101001

This review comes from a themed issue on **Electrocatalysis**

Edited by **Nicolas Alonso-Vante**

For a complete overview see the [Issue](#) and the [Editorial](#)

Available online 4 April 2022

<https://doi.org/10.1016/j.coelec.2022.101001>

2451-9103/© 2022 The Author(s). Published by Elsevier B.V. This is an open access article under the CC BY license (<http://creativecommons.org/licenses/by/4.0/>).

**Keywords**

Water splitting, Metal dichalcogenide, Hydrogen evolution reaction, Electrolysis, 2D materials.

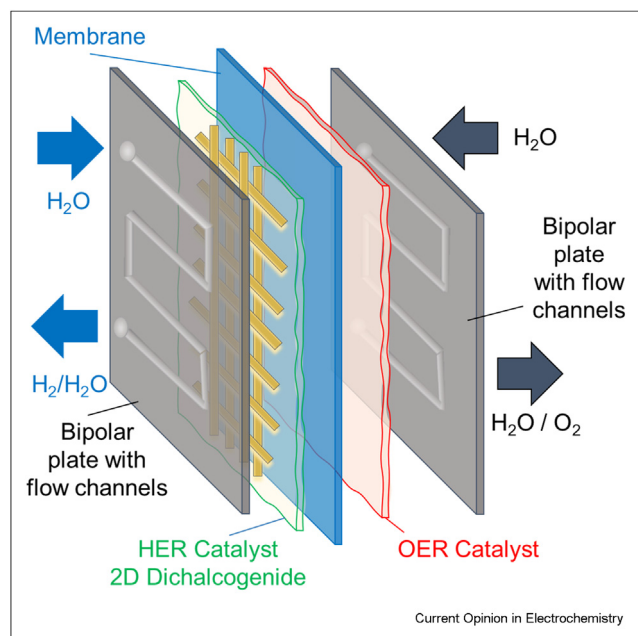
## Introduction to metal dichalcogenides as hydrogen evolution electrocatalysts

Electrochemical devices will play a central role in facilitating a future powered by renewable energy

sources, by allowing this energy to be stored to mitigate for the peaks and troughs in supply that characterize renewables [1]. Electrolyzers that split water into hydrogen and oxygen constitute one class of electrochemical technology that will be especially important in this regard, as hydrogen is an excellent fuel [2]. Moreover, if the required electricity comes from a renewable energy source, H<sub>2</sub> can be generated at minimal cost to the environment and practically carbon-neutrally [3,4]. Of the various electrolyzer technologies that currently exist, proton exchange membrane electrolyzers (see [Figure 1](#)) are generally viewed as the most promising for integration with renewable power sources due to their fast start-up and shut-down times, which should give these devices a certain tolerance to intermittent renewable power inputs [5,6]. However, the proton exchange membrane in such electrolyzers imposes a very acidic environment on the cell components, in turn requiring electrocatalysts that are stable at low pH. Typically, precious metals are the catalysts of choice: IrO<sub>2</sub> and RuO<sub>2</sub> at the anode and dispersed Pt at the cathode [7]. However, although highly catalytically active, such precious metal catalysts are rare, expensive and add considerably to the lifecycle carbon assessment of the electrolyzer; for example, producing 1 g of Pt produces ~33 kg of CO<sub>2</sub> equivalents [8].

For these reasons, minimizing the amount of Pt used in electrolyzers, or indeed replacing Pt entirely, is a major area of study at the current time [9,10]. In this regard, two-dimensional (2D) transition metal chalcogenides are exciting candidates for the role of hydrogen evolution electrocatalysts in proton exchange membrane electrolyzers for a number of reasons. Firstly, recent evidence suggests that the stability of these materials as hydrogen evolution electrocatalysts in acidic solution is similar to that of Pt, thus allowing them to compete with Pt in terms of durability [11]. Secondly, they can be deposited as continuous and robust thin films directly onto gas diffusion layers (or other suitable supports) in proton exchange membrane electrolyzers, potentially negating the need to deposit catalysts onto the membrane itself [12–14]. Finally, 2D dichalcogenides are fascinating from a fundamental point of view because, unlike nanoparticles (where the catalytic processes may happen at a range of surfaces, faces and edges), the orientation of

Figure 1



A schematic of a single cell proton exchange membrane electrolyzer. Dichalcogenide electrocatalysts can be deposited directly onto the porous gas diffusion layer (yellow grid in the figure) to maximize catalytic surface area. A typical device operates with a rapid flow of water and at temperatures  $\approx 60\text{--}70\text{ }^\circ\text{C}$ , requiring extremely robust materials. OER = oxygen evolution reaction; HER = hydrogen evolution reaction.

a 2D transition metal chalcogenide (film) is always precisely defined with respect to the substrate (Figure 2). Since the (001) lattice plane (commonly referred to as the basal plane) is the only interface participating in the hydrogen evolution reaction, there is no possibility for complications or ambiguity regarding selection of the optimal surface for hydrogen evolution [15].

In this minireview, we aim to give an overview of metallically-conductive 2D dichalcogenides reported since 2019 which show catalytic activity for the hydrogen evolution reaction from their basal plane sites, on account of these materials being the most promising for applications in proton exchange membrane electrolyzers. In doing so, we have intentionally selected reports which specified their materials' sizes and morphologies in order to make sure that any catalytic activity from edge sites can be neglected (recent work has indicated that the degradation of 2D dichalcogenides proceeds rapidly on the edge sites [16]). We have also chosen to avoid discussion of nanostructured materials due to the complexity of this subject (which would require significantly more space than available in this minireview to cover in adequate detail). Readers interested in nanostructured metal dichalcogenides for electrochemical energy conversion are directed to a number of excellent review articles on this subject [17–19].

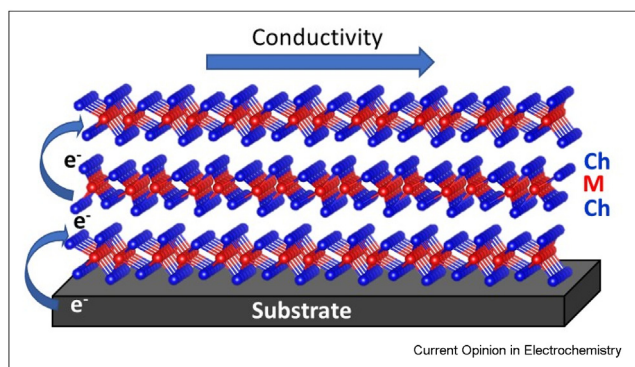
In choosing the examples we discuss below, we operate under the notion that continuous and defect-free films of dichalcogenides with intrinsically high electrical conductivity have the best prospects for withstanding interaction with the required water flow under the extremely reducing conditions prevailing at the cathode of a proton exchange membrane electrolyzer, and therefore, the best prospects for competing with Pt in a practical device. Table 1 summarizes data from research articles published since 2019 in which predominantly defect-free samples (with mainly the basal plane exposed) were studied for the electrochemical hydrogen evolution reaction, and which we will discuss further below. For comparison, Table 1 also includes entries for Pt and  $\text{Ni}_2\text{P}$  as alternative hydrogen evolution electrocatalysts.

### The hydrogen evolution reaction on the basal plane of group 5 dichalcogenides

The Group 5 dichalcogenides ( $\text{VTe}_2$ ,  $\text{TaS}_2$ ,  $\text{TaSe}_2$ ,  $\text{NbS}_2$ ) might seem to be obvious choices as electrocatalysts for the hydrogen evolution reaction as they tend to show metallic conductivity in their stable crystal forms. Highly crystalline hexagonal  $\text{TaS}_2$  flakes produced by exfoliation of single crystals (shown to be phase-pure by X-ray and electron diffraction studies, and with a nearly perfect Ta: S ratio of 1 : 2 according to XPS (X-ray photoelectron spectroscopy)) exhibits a relatively high overpotential requirement to achieve a current density of  $10\text{ mA cm}^{-2}$  for hydrogen evolution of 575 mV [20]. As the flakes had sufficiently large lateral sizes (Table 1, entry 1) this suggested that the activity stemmed from the basal planes. However, the authors noted the presence of up to 40% of a surface oxide ( $\text{Ta}_2\text{O}_5$ ) based on the presence of  $\text{Ta}^{5+}$  peaks in the XPS spectrum. This observation poses the question as to whether the formation of Ta nanoparticles is possible due to reduction of  $\text{Ta}_2\text{O}_5$ . The challenge of keeping crystals free from oxides was further confirmed by recent electrochemical studies on  $\text{TaS}_2$  and  $\text{TaSe}_2$  crystals which showed a significant presence of  $\text{Ta}_2\text{O}_5$  (Table 1, entries 2 and 3) [21]. The identical overpotentials (390 mV) required to deliver current densities of  $10\text{ mA cm}^{-2}$  for hydrogen evolution for  $\text{TaS}_2$  and  $\text{TaSe}_2$  indicate that oxides may play a determining role in electrochemical performance, further suggesting that  $\text{TaS}_2$  is unlikely to be an ideal material for the hydrogen evolution reaction.

$\text{NbS}_2$  is an interesting target since the flakes can be grown directly on carbon cloth by chemical vapor deposition (CVD) from  $\text{NbCl}_5$  and sulfur sources. The resulting  $\text{NbS}_2$  flakes with lateral sizes of  $1 \times 1\text{ }\mu\text{m}^2$  oriented in-plane with the carbon cloth fibres delivered hydrogen evolution at  $10\text{ mA cm}^{-2}$  with  $\eta = 453\text{ mV}$  [14] (Table 1, entry 4). These results are however in stark contrast with a recent report on  $\text{NbS}_2$  showing a respectable overpotential demand of only  $\approx 290\text{ mV}$  in

Figure 2



A typical three-layer structural motif in a metallic 2D-dichalcogenide consisting of edge-sharing distorted  $\{MCh_6\}$  octahedra with the layers parallel to the substrate. The top (001) layer is often referred to as the basal plane. The conductivity is greater in-plane than perpendicular to the plane. A reduced number of planes may lead to lower Ohmic losses in an electrochemical cell. Usual performance criteria are based on electronic conductivity, structural integrity, and abundance of active sites. M = metal; Ch = chalcogenide.

order to achieve  $10 \text{ mA cm}^{-2}$  [22]. In addition, Yang et al. reported a significant decrease in the required overpotential for non-stoichiometric  $Nb_{1.35}S_2$  from *ca.* 290 mV to 123 mV and a Tafel slope of just 43 mV/decade. Current densities of more than  $5000 \text{ mA cm}^{-2}$  were observed as well, contradicting earlier reports that showed that non-stoichiometric  $NbS_{1.6}$  ( $Nb_{1.25}S_2$ ) could not reach current densities even as low as  $10 \text{ mA cm}^{-2}$

[31]. A possible explanation could be differences in material morphology. It appears that the utilization of atomically thin ( $< 20 \text{ nm}$ ) flakes may play an important role due to improved electron transfer from the substrate (Figure 2) [22]; reducing the layer thickness may be a way to challenge the poor catalytic ability of Group 5 dichalcogenides [31].

The role of layer thickness seems to be further confirmed by recent work on  $1T'-VTe_2$  flakes with  $\approx 30 \text{ nm}$  thickness, which required  $\eta = 220 \text{ mV}$  at  $10 \text{ mA cm}^{-2}$  (with a Tafel slope of 40 mV/decade) [24]. In comparison, a significantly higher overpotential requirement to reach  $10 \text{ mA cm}^{-2}$  (441 mV) and a higher Tafel slope (70 mV/decade) were previously reported on bulk  $VTe_2$  crystals [23] (Table 1, entries 6 and 7).

### The hydrogen evolution reaction on the basal plane of group 6 dichalcogenides

Arguably, no review is complete without mentioning metallic  $1T-MoS_2$  and  $1T-WS_2$  phases, which to-date are probably the most explored 2D dichalcogenides for the hydrogen evolution reaction following on from their first reports almost a decade ago [32–34]. Despite complex synthesis procedures which involve butyllithium-aided exfoliation, they appear as very competent hydrogen evolution electrocatalysts, with  $\eta$  for  $1T-MoS_2$  as low as 250 mV at  $10 \text{ mA cm}^{-2}$  reported (Table 1, entry 8) [22]. However, there is an important underlying issue with both of these dichalcogenides: they are metastable and tend to revert rapidly into semiconducting and

Table 1

An overview of 2D transition metal dichalcogenides tested in acidic conditions for the hydrogen evolution reaction reported since 2019.  $\eta$  = overpotential. All electrolytes are 0.5 M  $H_2SO_4$  except entry 4 (0.05 M  $H_2SO_4$ ).

Entry	Electrode	Basal plane surface dimensions	$\eta$ (mV) at $10 \text{ mA cm}^{-2}$	Tafel slope (mV/dec)	Substrate	Reference
1	2H-TaS <sub>2</sub>	$0.3 \times 0.4 \mu\text{m}^2$ flakes	575	>100	Glassy carbon button	[20]
2	2H-TaS <sub>2</sub>	$0.1 \times 0.1 \mu\text{m}^2$ flakes	390	–	Glassy carbon	[21]
3	2H-TaSe <sub>2</sub>	$0.1 \times 0.1 \mu\text{m}^2$ flakes	390	–	Glassy carbon	[21]
4	2H-NbS <sub>2</sub>	$1 \times 1 \mu\text{m}^2$ flakes	453	125	Carbon paper	[14]
5	2H-NbS <sub>2</sub>	$1 \times 2 \mu\text{m}^2$ flakes	$\approx 290$	140	Glassy carbon button	[22]
6	1T-VTe <sub>2</sub>	Single crystal	441	70	Au covered Si/SiO <sub>2</sub>	[23]
7	1T-VTe <sub>2</sub>	$50 \times 40 \mu\text{m}^2$ flakes	220	$\approx 40$	Glassy carbon	[24]
8	1T-MoS <sub>2</sub>	$1 \times 1 \mu\text{m}^2$ flakes	$\approx 250$	50	Glassy carbon button	[22]
9	1T-MoS <sub>2</sub>	$0.1 \times 0.1 \mu\text{m}^2$ flakes	352	72	Carbon paper	[25]
10	1T-WS <sub>2</sub>	$1 \times 1 \mu\text{m}^2$ flakes	$\approx 210$	48	Glassy carbon button	[22]
11	1T'-MoTe <sub>2</sub>	$1 \times 2 \mu\text{m}^2$ flakes	340	78	Glassy carbon button	[26]
12	1T'-MoTe <sub>2</sub>	Thin films	481	67	$1 \text{ cm}^2$ pyrolytic carbon	[12]
13	1T'-MoTe <sub>2</sub>	Thin films	$> 900^a$	392	$0.3 \times 0.5 \text{ cm}^2$ on Cu	[27]
14	1T'-MoTe <sub>2</sub>	Single crystal	480	–	$0.01 \text{ cm}^2$ crystal on Cu wire	[28]
15	1T'-MoTe <sub>2</sub>	Single crystal	668	137	Au covered Si/SiO <sub>2</sub>	[23]
16	1T'-WTe <sub>2</sub>	$10 \times 10 \mu\text{m}^2$ flakes	450	238	Au covered Si/SiO <sub>2</sub>	[29]
17	1T'-WTe <sub>2</sub>	Single crystal	692	169	Au covered Si/SiO <sub>2</sub>	[23]
18	Pt	N/A	$\sim 30$	30	N/A	[30]
19	Ni <sub>2</sub> P	N/A	150	46	Ti foil	[30]

<sup>a</sup> At a current density of  $4 \text{ mA cm}^{-2}$ .



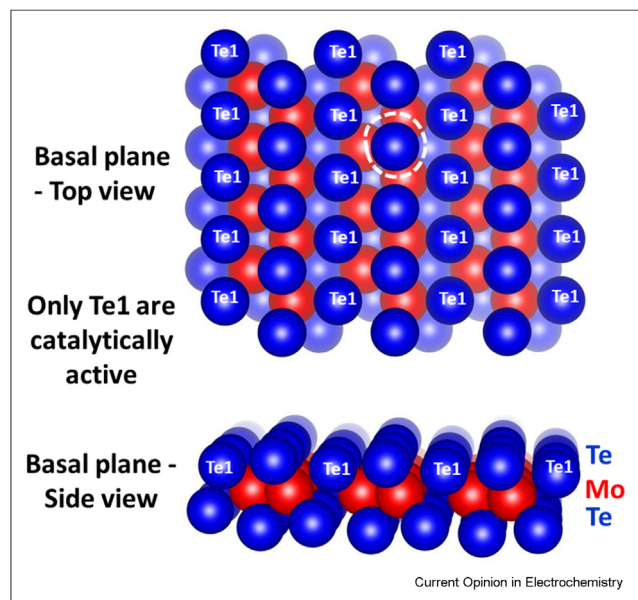
effectively non-catalytic materials over time, with this conversion rapidly accelerated at temperatures as low as 80 °C [25]. Given that typical proton exchange membrane electrolyzers operate at  $\approx 60\text{--}70$  °C [35], both 1T-MoS<sub>2</sub> and WS<sub>2</sub> probably make poor choices as electrode materials in practical devices. Intercalation of phenanthroline into layered 1T-MoS<sub>2</sub> has been shown to slow the transformation with only moderate increase in the overpotential requirement, from 352 to 383 mV at 10 mA cm<sup>-2</sup> [25]. Furthermore, computational studies also suggest that intercalation of small molecules into 1T'-MoS<sub>2</sub> may improve its stability [36]. However, this could prove complex to implement at large scale, and so the practicality of such an approach for electrocatalysts in real-world devices remains to be established.

Given the challenges associated with MoS<sub>2</sub> and WS<sub>2</sub>, metallic 1T'-MoTe<sub>2</sub> has become a rather popular alternative (Figure 3). Despite the fact that only 50% of the Te centres at the surface have sufficiently low hydrogen adsorption energies, single crystals (*ca.* 1 × 2 μm<sup>2</sup> in size) displayed  $\eta$  for 10 mA cm<sup>-2</sup> as low as 340 mV (Table 1, entry 11), which suggests that the catalytic activity originates from the basal plane [26]. A key advantage of MoTe<sub>2</sub> is the simplicity with which thin films of this material can be grown selectively on various substrates [37]. However, the evaluation of metallic 1T'-MoTe<sub>2</sub> films deposited and measured directly on the 1 cm<sup>2</sup> scale revealed a much higher overpotential requirement of 481 mV at 10 mA cm<sup>-2</sup> [12]. These high overpotential values are in line with work by Zhuang et al. [27], which showed that a film of MoTe<sub>2</sub>

transferred onto Cu foil could only achieve a current density of 4 mA cm<sup>-2</sup> at  $\eta > 900$  mV (Table 1, entry 13). However, as the initial film was grown by a CVD process and later transferred onto the Cu-substrate, the oxidation of the film surface during this transfer could not be completely excluded. In addition, the hydrophobic nature of 1T'-MoTe<sub>2</sub> films [38] could also be a factor inhibiting catalysis. This highlights the challenges associated with implementation of chalcogenides in practical applications, especially as they seem to be quite prone to surface oxidation. This hypothesis is borne out by recent work on a high-quality single crystal of 1T'-MoTe<sub>2</sub> [28], which reported an overpotential value of 480 mV at 10 mA cm<sup>-2</sup> (more in line with the values found by McManus et al. in films of this material [12]).

The already mentioned low energy of adsorption seems to be quite evident from the Tafel slopes of the majority of the 1T'-MoTe<sub>2</sub> samples, which tend to gravitate towards 120 mV/decade, suggesting that the effective adsorption of protons at the surface (the Volmer process) is the reaction limiting step [39]. Inducing vacancies in the material has been suggested as effective way of reducing of the energy of adsorption to 0.21 eV [23]. This may give some clue as to why there is such variation in electrochemical performance observed for the metallic MoTe<sub>2</sub> samples across the literature. If there are a small number of vacancies, especially on non-catalytic sites (highlighted as the white dashed circle in Figure 3), this may lead to improved performance, and this may in turn provide an explanation for the observation that, upon prolonged cycling, 1T'-MoTe<sub>2</sub> shows a gradual reduction of the overpotential requirement to achieve 10 mA cm<sup>-2</sup> from 320 to 170 mV [40] (or 340 to 261 mV at the same current density in single crystals [26]). However, the presence of vacancies is not necessarily the only explanation. It has been suggested that this improvement in performance could be a purely electronic phenomenon due to doping of electrons into the topological structure [26,28]. The change in Tafel slope from 68 to 117 mV/decade does, however, indicate that prolonged cycling may lead to the elimination of the surface oxide and that the lower overpotentials may in fact be displayed by pure 1T'-MoTe<sub>2</sub>. As mentioned above, DFT simulations have shown a relatively high energy of adsorption of H<sup>+</sup> on the surface of MoTe<sub>2</sub>. Therefore, the change to a higher Tafel slope, alongside decreased overpotential, seem to support this hypothesis. Still, whether it is electron doping, removal of an oxide layer, or the presence of vacancies that drives this activation process, it is currently unclear as to the effects of any of these on the integrity of the films. Careful experiments under inert conditions are required in order to uncover the full details of this reduction in overpotential. More investigation in practical conditions (*e.g.* flow-cells) would also be useful; studies so far have shown that MoTe<sub>2</sub> remains stable (up to current

Figure 3



The basal plane of 1T'-MoTe<sub>2</sub> (a typical metallic dichalcogenide). Only 50% of the Te atoms are active. The white dashed circle highlights the Te atom that could be removed to drive the improvement in catalytic ability.

densities of  $250 \text{ mA cm}^{-2}$ ) during prolonged bulk electrolysis and cycling for at least 1000 scans, as confirmed by analysis of the electrolyte [26].

Finally,  $\text{WTe}_2$  is the only Group 6 dichalcogenide for which the metallic state is always stable and so there is no ambiguity as to whether a tiny impurity of the semiconducting phase may have been the cause for any deterioration in performance. The study of  $10 \times 10 \mu\text{m}^2$  flakes (identified as single phase by X-ray diffraction and Raman spectroscopy) on Au electrodes revealed  $\eta = 450 \text{ mV}$  at a current density of  $10 \text{ mA cm}^{-2}$  [29]. This is around 250 mV lower than similar studies on larger single crystals (Table 1, entries 16 and 17), indicating that non-stoichiometry and the possible presence of edge sites plays an important role in catalytic performance in the  $\text{WTe}_2$  system [23].

## Conclusions and outlook

In this minireview, we have given a short overview of some of the more recent developments in the field of 2D metal dichalcogenides as hydrogen evolution electrocatalysts, especially in the context of applying these materials in proton exchange membrane electrolyzers. Although their overpotential metrics for hydrogen production are worse than those of Pt, 2D metal dichalcogenides are generally less scarce than Pt and production of their metallic components incurs considerably lower global warming potential (e.g.  $\sim 12 \text{ kg}$  of  $\text{CO}_2$  equivalents per kg of Nb and 260 kg of  $\text{CO}_2$  equivalents per kg of Ta, both of which values are several orders of magnitude lower than for Pt [41]). 2D metal dichalcogenides and their components are also considerably cheaper and more abundant than Pt [42]. These factors will be important in the context of powering electrolyzers at low current densities using renewable energy sources [43]. Such low current density conditions can tolerate less effective electrocatalysts and it may well make sense to employ higher loadings of cheaper materials in such contexts, rather than Pt. Finding materials that can be deployed at high loading and which form continuous, robust thin films on high surface area substrates is therefore a very attractive target for facilitating electrochemical renewables-to-hydrogen conversion. 2D metal dichalcogenides fit this profile very well, and recent theoretical work indicates that the nature of the substrate may have a distinct effect on the electronic and catalytic properties of various 2D metal dichalcogenides [44], with implications for how these materials might be deployed (direct deposition on gas diffusion layers in a “catalyst-coated substrate” approach [45] being a possibility [37]).

In terms of the immediate opportunities and challenges in the field, exact information about the nature of the surface offers exciting prospects for computational research, allowing rapid screening of the properties of a broad range of chalcogenides and predictions of catalytic

performance [46,47]. Being able to predict with confidence whether a particular 2D chalcogenide is catalytically active or not would be a major boon to innovation. Meanwhile, finding the right balance between the durability of 2D metal dichalcogenide films and the number of induced defects will be crucial for real-world applications; in this regard applying high-throughput flow cells and bespoke micro-reactors for in-depth analysis of these materials *in operando* will be essential [48,49]. Finally, these materials must then be incorporated into scaled-up electrolyzer devices and their performance monitored over extended time periods. Through efforts such as these, the tremendous potential of 2D metal dichalcogenides to act as low-cost electrocatalysts for the production of hydrogen from water driven by renewable energy will come closer to being realized.

## Declaration of competing interest

The authors declare that they have no known competing financial interests or personal relationships that could have appeared to influence the work reported in this article.

## Acknowledgments

The authors thank the EPSRC for funding (EP/N509668/1 and EP/R20914/1) and MDS thanks the Royal Society for a University Research Fellowship (UF150104).

## References

Papers of particular interest, published within the period of review, have been highlighted as:

- \* of special interest
- \*\* of outstanding interest

1. Maddukuri S, Malka D, Chae MS, Elias Y, Luski S, Aurbach D: **On the challenge of large energy storage by electrochemical devices.** *Electrochim Acta* 2020, **354**:136771, <https://doi.org/10.1016/j.electacta.2020.136771>.
2. Wallace JS, Ward CA: **Hydrogen as a fuel.** *Int J Hydrogen Energy* 1983, **8**:255–268, [https://doi.org/10.1016/0360-3199\(83\)90136-2](https://doi.org/10.1016/0360-3199(83)90136-2).
3. Bareiß K, la Rua C, Möckl M, Hamacher T: **Life cycle assessment of hydrogen from proton exchange membrane water electrolysis in future energy systems.** *App Energy* 2019, **237**: 862–872, <https://doi.org/10.1016/j.apenergy.2019.01.001>.
4. Osman AI, Mehta N, Elgarahy AM, Hefny M, Al-Hinai A, Al-Muhtaseb AH, Rooney DW: **Hydrogen production, storage, utilisation and environmental impacts: a review.** *Environ Chem Lett* 2022, **20**:153–188, <https://doi.org/10.1007/s10311-021-01322-8>.
5. Weiß A, Siebel A, Bernt M, Shen T-H, Tileli V, Gasteiger HA: **Impact of intermittent operation on lifetime and performance of a PEM water electrolyzer.** *J Electrochem Soc* 2019, **166**: F487, <https://doi.org/10.1149/2.0421908jes>.
6. Escobar-Yonoff R, Maestre-Cambonel D, Charry S, Rincón-Montenegro A, Portnoy I: **Performance assessment and economic perspectives of integrated PEM fuel cell and PEM electrolyzer for electric power generation.** *Heliyon* 2021, **7**, e06506, <https://doi.org/10.1016/j.heliyon.2021.e06506>.
7. Hinsen JN, Prats H, Toudahl KK, Secher NM, Chan K, Kibsgaard J, Chorkendorff I: **Is there anything better than Pt for HER?** *ACS Energy Lett* 2021, **6**:1175–1180, <https://doi.org/10.1021/acsenergylett.1c00246>.

8. Mori M, Stropnik R, Sekavčnik M, Lotrič A: **Criticality and life-cycle assessment of materials used in fuel-cell and hydrogen technologies.** *Sustainability* 2021, **13**:3565, <https://doi.org/10.3390/su13063565>.
- A comprehensive life cycle assessment of the components of a proton exchange membrane electrolyzer, highlighting the often hidden environmental costs of some key components (including precious metal electrocatalysts).
9. Roger I, Shipman MA, Symes MD: **Earth-abundant catalysts for electrochemical and photoelectrochemical water splitting.** *Nat Rev Chem* 2017, **1**:3, <https://doi.org/10.1038/s41570-016-0003>.
10. Hubert MA, King LA, Jaramillo TF: **Evaluating the case for reduced precious metal catalysts in proton exchange membrane electrolyzers.** *ACS Energy Lett* 2022, **7**:17–23, <https://doi.org/10.1021/acsenergylett.1c01869>.
11. Wang Z, Zheng Y-R, Montoya J, Hochfilzer D, Cao A, Kibsgaard J, Chorkendorff I, Nørskov JK: **Origins of the instability of nonprecious hydrogen evolution reaction catalysts at open-circuit potential.** *ACS Energy Lett* 2021, **6**:2268–2274, <https://doi.org/10.1021/acsenergylett.1c00876>.
- The dissolution of several promising non-precious catalysts (including the archetypal chalcogenide MoS<sub>2</sub>) was studied under reductive potentials in acidic solution, revealing that MoS<sub>2</sub> is at least as stable as Pt under these conditions.
12. McManus JB, Cunningham G, McEvoy N, Cullen CP, Gity F, Schmidt M, McAteer D, Mullarkey D, Shvets IV, Hurley PK, Hallam T, Duesberg GS: **Growth of 1T' MoTe<sub>2</sub> by thermally assisted conversion of electrodeposited tellurium films.** *ACS Appl Energy Mater* 2019, **2**:521–530, <https://doi.org/10.1021/acsaem.8b01540>.
13. Lu D, Ren X, Ren L, Xue W, Liu S, Liu Y, Chen Q, Qi X, Zhong J: **Direct vapor deposition growth of 1T' MoTe<sub>2</sub> on carbon cloth for electrocatalytic hydrogen evolution.** *ACS Appl Energy Mater* 2020, **3**:3212–3219, <https://doi.org/10.1021/acsaem.9b01589>.
14. Kumar H, Wang K, Tang F, Zeng X, Gan L, Su Y: **Unveiling active sites by structural tailoring of two-dimensional niobium disulfide for improved electrocatalytic hydrogen evolution reaction.** *Int J Energy Res* 2020, **44**:10551–10561, <https://doi.org/10.1002/er.5691>.
15. Sun Y, Wang L, Guselnikova O, Semyonov O, Fraser J, Zhou Y, López N, Ganin AY: **Revealing the activity of Co<sub>3</sub>Mo<sub>3</sub>N and Co<sub>3</sub>Mo<sub>3</sub>N<sub>0.5</sub> as electrocatalysts for the hydrogen evolution reaction.** *J Mater Chem A* 2022, **10**:855–861, <https://doi.org/10.1039/D1TA08389A>.
16. Tao B, Unwin PR, Bentley CL: **Nanoscale variations in the electrocatalytic activity of layered transition-metal dichalcogenides.** *J Phys Chem C* 2020, **124**:789–798, <https://doi.org/10.1021/acs.jpcc.9b10279>.
17. Wu X, Zhang H, Zhang J, Lou XW: **Recent advances on transition metal dichalcogenides for electrochemical energy conversion.** *Adv Mater* 2021, **33**:2008376, <https://doi.org/10.1002/adma.202008376>.
18. Giuffredi G, Di Fonzo F: **Disorder engineering in transition metal dichalcogenides toward efficient high current density reduction electrocatalysts.** *Curr Opin Electrochem* 2021, **25**:100639, <https://doi.org/10.1016/j.coelec.2020.09.006>.
19. Li Z, Yue Y, Peng J, Luo Z: **Phase engineering two-dimensional nanostructures for electrocatalytic hydrogen evolution reaction.** *Chin Chem Lett* 2022, <https://doi.org/10.1016/j.ccllet.2022.01.012>.
20. Kovalska E, Roy PK, Antonatos N, Mazanek V, Vesely M, Wu B, Sofer Z: **Photocatalytic activity of twist-angle stacked 2D TaS<sub>2</sub>.** *NPJ 2D Mater* 2021, **5**:68, <https://doi.org/10.1038/s41699-021-00247-8>.
- By demonstrating that exposure of large TaS<sub>2</sub> flakes to different wavelengths of light improves catalytic activity, the authors went a step beyond a simple investigation of electrocatalytic hydrogen evolution.
21. Najafi L, Bellani S, Oropesa-Nuñez R, Martín-García B, Prato M, Pasquale L, Panda J-K, Marvan P, Sofer Z, Bonaccorso F: **TaS<sub>2</sub>, TaSe<sub>2</sub>, and their heterogeneous films as catalysts for the hydrogen evolution reaction.** *ACS Catal* 2020, **10**:3313–3325, <https://doi.org/10.1021/acscatal.9b03184>.
22. Yang J, Mohamad AR, Wang Y, Fullon R, Song X, Zhao F, Bozkurt I, Augustin M, Santos EJJ, Shin HS, Zhang W, Voiry D, Jeong HY, Chhowalla M: **Ultra-high-current-density niobium disulfide catalysts for hydrogen evolution.** *Nat Mater* 2019, **18**:1309–1314, <https://doi.org/10.1038/s41563-019-0463-8>.
23. Kwon H, Bae D, Jun H, Ji B, Won D, Lee J-H, Son Y-W, Yang H, Cho S: **Basal-plane catalytic activity of layered metallic transition metal ditellurides for the hydrogen evolution reaction.** *Appl Sci* 2020, **10**:3087, <https://doi.org/10.3390/app10093087>.
- A comprehensive and technically perfect work on single crystals of three key metallic dichalcogenides (MoTe<sub>2</sub>, VTe<sub>2</sub> and WTe<sub>2</sub>) allowing them to be benchmarked against each other.
24. Shi J, Huan Y, Zhao X, Yang P, Hong M, Xie C, Pennycook S, Zhang Y: **Two-dimensional metallic vanadium ditelluride as a high-performance electrode material.** *ACS Nano* 2021, **15**:1858–1868, <https://doi.org/10.1021/acsnano.0c10250>.
25. Goloveshkin AS, Lenenko ND, Naumkin AV, Pereyaslavtsev AY, Grigorieva AV, Shapovalov AV, Talanova VN, Polezhaev AV, Zaikovskii VI, Novikov VV, Korlyukov AA, Golub AS: **Enhancement of 1T-MoS<sub>2</sub> superambient temperature stability and hydrogen evolution performance by intercalating a phenanthroline monolayer.** *ChemNanoMat* 2021, **7**:447–456, <https://doi.org/10.1002/cnma.202000586>.
26. McGlynn JC, Dankwort T, Kienle L, Bandeira NAG, Fraser JP, Gibson EK, Cascallana-Matías I, Kamarás K, Symes MD, Miras HN, Ganin AY: **The rapid electrochemical activation of MoTe<sub>2</sub> for the hydrogen evolution reaction.** *Nat Commun* 2019, **10**:4916, <https://doi.org/10.1038/s41467-019-12831-0>.
27. Zhuang P, Sun Y, Dong P, Smith W, Sun Z, Ge Y, Pei Y, Cao Z, Ajayan PM, Shen J, Ye M: **Revisiting the role of active sites for hydrogen evolution reaction through precise defect adjusting.** *Adv Funct Mater* 2019, **29**:1901290, <https://doi.org/10.1002/adfm.201901290>.
28. Katz RJ, Zhu Y, Mao Z, Schaak RE: **Persistence and evolution of materials features during catalysis using topological and trivial polymorphs of MoTe<sub>2</sub>.** *ChemCatChem* 2021, **14**:e202101714, <https://doi.org/10.1002/cctc.202101714>.
- A beautifully-executed work on single crystals of MoTe<sub>2</sub> demonstrating that topological surface characteristics of the telluride are unaffected by electrolysis, suggesting that the material can produce hydrogen effectively even when covered with a layer of oxide.
29. Yang H, Zhao Y, Wen Q, Yang R, Liu Y, Li H, Zhai T: **Single WTe<sub>2</sub> sheet-based electrocatalytic microdevice for directly detecting enhanced activity of doped electronegative anions.** *ACS Appl Mater Interfaces* 2021, **13**:14302–14311, <https://doi.org/10.1021/acsmi.1c01091>.
30. Popczun EJ, McKone JR, Read CG, Biacchi AJ, Wiltrout AM, Lewis NS, Schaak RE: **Nanostructured nickel phosphide as an electrocatalyst for the hydrogen evolution reaction.** *J Am Chem Soc* 2013, **135**:9267–9270. [dx.doi.org/10.1021/ja403440e](https://doi.org/10.1021/ja403440e).
31. Chia X, Ambrosi A, Lazar P, Soferc Z, Pumera M: **Electrocatalysis of layered Group 5 metallic transition metal dichalcogenides (MX<sub>2</sub>, M = V, Nb, and Ta; X = S, Se, and Te).** *J Mater Chem A* 2016, **4**:14241–14253, <https://doi.org/10.1039/C6TA05110C>.
32. Lukowski MA, Daniel AS, Meng F, Forticaux A, Li L, Jin S: **Enhanced hydrogen evolution catalysis from chemically exfoliated metallic MoS<sub>2</sub> nanosheets.** *J Am Chem Soc* 2013, **135**:10274–10277, <https://doi.org/10.1021/ja404523s>.
33. Voiry D, Yamaguchi H, Li J, Silva R, Alves DCB, Fujita T, Chen M, Asefa T, Shenoy VB, Eda G, Chhowalla M: **Enhanced catalytic activity in strained chemically exfoliated WS<sub>2</sub> nanosheets for hydrogen evolution.** *Nat Mater* 2013, **12**:850–855, <https://doi.org/10.1038/nmat3700>.
34. Voiry D, Salehi M, Silva R, Fujita T, Chen M, Asefa T, Shenoy VB, Eda G, Chhowalla M: **Conducting MoS<sub>2</sub> nanosheets as catalysts for hydrogen evolution reaction.** *Nano Lett* 2013, **13**:6222–6227, <https://doi.org/10.1021/nl403661s>.



35. Carmo M, Fritz DL, Mergel J, Stolten D: **A comprehensive review on PEM water electrolysis**. *Int J Hydrogen Energy* 2013, **38**:4901–4934, <https://doi.org/10.1016/j.ijhydene.2013.01.151>.
36. Chen J, Li F, Tang Y, Tang Q: **Tuning the phase stability and surface HER activity of 1T'-MoS<sub>2</sub> by covalent chemical functionalization**. *J Mater Chem C* 2020, **8**:15852–15859, <https://doi.org/10.1039/D0TC03943H>.
37. Fraser JP, Masaityte L, Zhang J, Laing S, Moreno-López JC, McKenzie AF, McGlynn JC, Panchal V, Graham D, Kazakova O, Pichler T, MacLaren DA, Moran DAJ, Ganin AY: **Selective phase growth and precise-layer control in MoTe<sub>2</sub>**. *Commun Mater* 2020, **1**:48, <https://doi.org/10.1038/s43246-020-00048-4>.
38. Fraser JP, Postnikov P, Miliutina E, Kolska Z, Valiev R, Švorčík V, Lyutakov O, Ganin AY, Guseynikova O: **Application of a 2D molybdenum telluride in SERS detection of biorelevant molecules**. *ACS Appl Mater Interfaces* 2020, **12**:47774–47783, <https://doi.org/10.1021/acsami.0c11231>.
39. Shinagawa T, Garcia-Esparza AT, Takanabe K: **Insight on Tafel slopes from a microkinetic analysis of aqueous electrocatalysis for energy conversion**. *Sci Rep* 2015, **5**:13801, <https://doi.org/10.1038/srep13801>.
40. McGlynn JC, Friskey M, Ganin AY: **Parameter optimisation for electrochemically activated MoTe<sub>2</sub>**. *Sustain Energy Fuels* 2020, **4**:4473–4477, <https://doi.org/10.1039/D0SE00684J>.
41. Nuss P, Eckelman MJ: **Life cycle assessment of metals: a scientific synthesis**. *PLOS ONE* 2014, **9**, e101298, <https://doi.org/10.1371/journal.pone.0101298>.
42. Schulz KJ, Piatak NM, Papp JF: **Niobium and tantalum, Critical mineral resources of the United States—economic and environmental geology and prospects for future supply: U.S. Geological survey professional paper 1802**. 2017M1–M34, <https://doi.org/10.3133/pp1802M>.
43. Chisholm G, Cronin L, Symes MD: **Decoupled electrolysis using a silicotungstic acid electron-coupled-proton buffer in a proton exchange membrane cell**. *Electrochim Acta* 2020, **331**: 135255, <https://doi.org/10.1016/j.electacta.2019.135255>.
44. Li F, Tang Q: **Modulating the electronic structure and in-plane activity of two-dimensional transition metal dichalcogenide (MoS<sub>2</sub>, TaS<sub>2</sub>, NbS<sub>2</sub>) monolayers by interfacial engineering**. *J Phys Chem C* 2020, **124**:8822–8833, <https://doi.org/10.1021/acs.jpcc.0c01094>.
45. Lim BH, Majlan EH, Tajuddin A, Husaini T, Daud WRW, Radzuan NAM, Haque MA: **Comparison of catalyst-coated membranes and catalyst-coated substrate for PEMFC membrane electrode assembly: a review**. *Chin J Chem Eng* 2021, **33**:1–16, <https://doi.org/10.1016/j.cjche.2020.07.044>.
46. Zhao N, Wang L, Zhang Z, Li Y: **Activating the MoS<sub>2</sub> basal planes for electrocatalytic hydrogen evolution by 2H/1T' structural interfaces**. *ACS Appl Mater Interfaces* 2019, **11**: 42014–42020, <https://doi.org/10.1021/acsami.9b11708>.
47. Gao B, Du X, Zhao Y, Cheon WS, Ding S, Xiao C, Song Z, Jang HW: **Electron strain-driven phase transformation in transition-metal-co doped MoTe<sub>2</sub> for electrocatalytic hydrogen evolution**. *Chem Eng J* 2021:133768, <https://doi.org/10.1016/j.cej.2021.133768>.
48. Lee Y, Ling N, Kim D, Zhao M, Eshete YA, Kim E, Cho S, Yang H: **Heterophase boundary for active hydrogen evolution in MoTe<sub>2</sub>**. *Adv Funct Mater* 2021:2105675, <https://doi.org/10.1002/adfm.202105675>.
49. Zhu X, Wang C, Fu L: **Engineering electrocatalytic microcells for two-dimensional materials**. *Cell Rep Phys Sci* 2020, **1**: 100190, <https://doi.org/10.1016/j.xcrp.2020.100190>.